

# Role of baryonic resonances in the dilepton emission in nucleon-nucleon collisions

R . Shyam and U . M osel

Institut für Theoretische Physik, Universität Giessen, D-35392 Giessen, Germany  
(April 4, 2019)

Within an effective Lagrangian model, we present calculations for cross sections of the dilepton production in proton-proton and proton-neutron collisions at laboratory kinetic energies in 1-5 GeV range. Production amplitudes include contributions from the nucleon-nucleon bremsstrahlung as well as from the mechanism of excitation, propagation, and radiative decay of  $\Delta(1232)$  and  $N(1520)$  intermediate baryonic resonances. It is found that the delta isobar term dominates the cross sections in the entire considered beam energy range. Our calculations are able to explain the data of the DLS collaboration on the dilepton production in proton-proton collisions for beam energies below 1.3 GeV. However, for incident energies higher than this the inclusion of contributions from other dilepton sources like Dalitz decay of  $\Delta^0$  and  $\Delta^+$  mesons, and direct decay of  $\Delta^0$  and  $\Delta^+$  mesons is necessary to describe the data.

25.75.D w, 13.30.C e, 12.40.Y x

On leave from Saha Institute of Nuclear Physics, Calcutta, India

## I. INTRODUCTION

Dileptons observed in the nucleus-nucleus collisions travel relatively unscathed from the production point to the detector. Therefore, they are expected to provide clear information about the early dense and hot stage of heavy ion collisions [1{3], which is in contrast to the hadronic probes which often suffer from strong final state interactions and the information about the collision history carried by them may be lost due to the rescattering in the expansion phase [4]. One of the phenomena predicted [5{13] at higher nuclear matter densities is the restoration of chiral symmetry which is manifested in the modification of masses of the vector mesons as a function of the nuclear matter density. Consequences of this effect can be observed in the dilepton ( $e^+ e^-$ ) spectra measured in nucleus-nucleus collisions [14]. More recently, enhancements observed in the measured [15,16] soft lepton pair production cross sections above known sources at the SPS energies, have also been attributed [17{21] to in-medium modifications of the vector meson properties rather than to creation of a new state of hadronic matter.

The investigation of the dilepton production in elementary nucleon-nucleon ( $N N$ ) collisions is of interest because the corresponding cross sections enter in the transport model calculations of the  $e^+ e^-$  spectra in the heavy ion collisions. Therefore, a quantitative understanding of this process is a natural prerequisite to an unequivocal determination of in-medium effects mentioned above. The study of this process is of interest in its own right as it is expected to provide deeper insight into the hadronic structure and the photon-hadron interactions. This investigation may give fundamental information on the electromagnetic form factor of the nucleon in the timelike region around the vector meson masses which is otherwise hard to access (see, e.g., [4]).

It has been known for some time that intermediate baryonic resonances play an important role in the dilepton production in the  $N N$  collisions. Dalitz decay of the isobar has been shown to be a strong dilepton production channel [22{24]. The importance of the baryonic resonance  $N^*(1520)$  has been emphasized for this process in Refs. [25,26] where it is pointed out that the subthreshold production (and its subsequent decay) via this resonance makes important contributions to the dilepton spectrum observed in the proton-proton ( $pp$ ) collisions. Therefore, the investigation of the dilepton production is expected to provide a useful tool to probe the parameters (e.g., coupling constants, form factors etc.) of the nucleon-resonance-photon vertices and masses and widths of the relevant nucleon resonances.

The aim of this paper is to investigate the dilepton production in nucleon-nucleon collisions in the beam energy range of 1-5 GeV within an effective Lagrangian model (ELM) which has been successfully applied to the description of pion and associated kaon production in  $pp$  collisions [27{29]. Initial interaction between two incoming nucleons is modeled by an effective Lagrangian which is based on the exchange of the  $\pi$ ,  $\rho$ ,  $\omega$ , and  $\rho'$  mesons. The coupling constants at the nucleon-nucleon-meson vertices are determined by directly fitting the  $T$  matrices of the nucleon-nucleon ( $N N$ ) scattering in the relevant energy region. The effective Lagrangian uses the pseudovector (PV) coupling for the nucleon-nucleon-pion vertex and thus incorporates the low energy theorems of current algebra and the hypothesis of PCAC. The  $e^+ e^-$  production proceeds via excitation, propagation and radiative decay of  $(1232)$  and  $N^*(1520)$  baryonic resonance states. Also included are the nucleon intermediate

ate states (which gives rise to the  $N\bar{N}$  bremsstrahlung contribution). The interference terms between various amplitudes are taken into account. The gauge invariance at the electromagnetic vertices is preserved in our calculations. Our model is similar in spirit to those of Refs. [24,30,31]. However, in Ref. [31] no resonance contribution was considered whereas in Ref. [24,30] resonance contributions were limited to the isobar only. The latter, though, did include the interference between the nucleon and terms. In calculations presented in Refs. [25,26,32],  $N\bar{N}$  bremsstrahlung contributions were ignored. We would like to stress that in Refs. [25,26] constant matrix elements have been used for various processes and the total dilepton production cross sections have been calculated by adding the corresponding cross sections and not the amplitudes, so part of the motivation of the present study is the investigation of the so far neglected quantum mechanical effects.

We investigate the role of baryonic resonances in the invariant mass spectrum of the dilepton produced in proton-proton and proton-neutron collisions at various beam energies in the 1-5 GeV range. To this end, we present the first full theoretic calculation of the dilepton production in  $N\bar{N}$  collisions where excitation, propagation and radiative decay of the  $N(1520)$  baryonic resonance are fully accounted for. We also compare our calculations with the published data [33] on the dilepton production in elementary proton-proton collisions, by the Dilepton Spectrometer (DLS) collaboration. In order to describe these data the contributions from other dilepton sources ( $^0$  and  $D$  decays and direct decay of  $^0$  and  $^1$  mesons) have also been considered.

The remainder of this paper is organized in the following way. Section II contains details of our theoretical approach. Section III comprises the results of our analysis and their discussions. The summary and conclusions of our work is presented in Sec. IV.

## II. FORMALISM

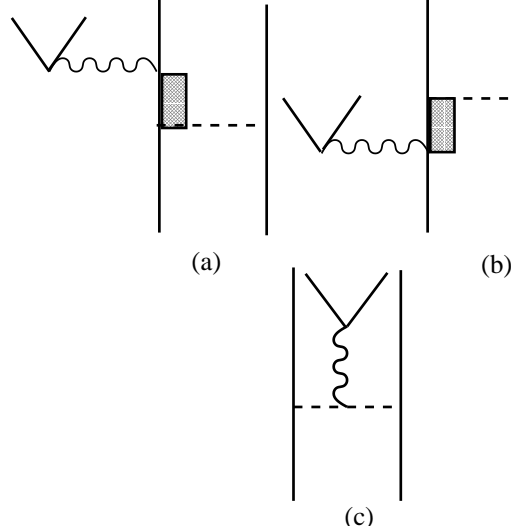


FIG. 1. A representative of Feynman diagrams for emission of dilepton in nucleon-nucleon collision as considered in this work. (a) denotes emission after  $N\bar{N}$  collision, (b) before  $N\bar{N}$  collision and (c) during  $N\bar{N}$  collision. The box represents any of an off-shell nucleon, a isobar or a  $N$  resonance.

A representative of the lowest order Feynman diagram contributing to the dilepton production as considered by us, is shown in Fig. 1. The intermediate nucleon or resonances can radiate a virtual photon which decays into a dilepton (Figs. 1a and 1b). There are also their exchange counterparts. In addition, there are diagrams of these types where the virtual photon is emitted from the nucleon line on the right side. The internal meson lines can also lead to dilepton emission (see Fig 1c). To evaluate various amplitudes, we have used the effective Lagrangians for the nucleon-nucleon-meson, resonance-nucleon-meson, nucleon-nucleon-photon and resonance-nucleon-photon vertices. These are discussed in the following subsections.

### A. Nucleon-nucleon-meson vertex

As done before in the investigation of  $p\bar{p} \rightarrow p\bar{p}^0$ ,  $p\bar{p} \rightarrow p\bar{n}^+$  [27] and  $p\bar{p} \rightarrow p\bar{K}^+$  [29] reactions, the parameters for these vertices are determined by fitting the  $N\bar{N}$  elastic scattering T matrix with an effective  $N\bar{N}$  interaction based on the  $\pi$ ,  $\rho$ ,  $\omega$ , and  $\rho'$  meson exchanges. The effective meson- $N\bar{N}$  Lagrangians are

$$L_{NN} = \frac{g_{NN}}{2m_N} \pi^5 \quad (\text{at } \pi^0) \quad : \quad (1)$$

$$L_{NN} = g_{NN} \pi^0 + \frac{k}{2m_N} \rho^0 \quad (\text{at } \rho^0) \quad : \quad (2)$$

$$L_{NN!} = g_{NN!} \pi^0 + \frac{k!}{2m_N} \omega^0 \quad (\text{at } \omega^0) \quad : \quad (3)$$

$$L_{NN} = g_{NN} \pi^0 \quad : \quad (4)$$

In Eqs. (1)–(4), we have used the notations and conventions of Bjorken and Drell [34] and definitions of various terms are the same as those given there. In Eq. (1)  $m_N$  denotes the nucleon mass. It should be noted that we use a PV coupling for the  $N\bar{N}$  vertex. Since these Lagrangians are used to directly model the  $N\bar{N}$  T matrix, we have also included a nucleon-nucleon-axial-vector-isovector vertex, with the effective Lagrangian given by

$$L_{NN\Lambda} = g_{NN\Lambda} \pi^5 \quad A ; \quad (5)$$

where  $A$  represents the axial-vector meson field. This term cures the unphysical behavior in the angular distribution of  $N\bar{N}$  scattering caused by the contact term in the one-pion exchange amplitude, if the mass of the axial meson  $A$  is chosen to be very large ( $\gg m_N$ ) [24].

At each interaction vertex, the following form factor is introduced

$$F_i^{NN} = \frac{\frac{2}{i} \frac{m_i^2}{q^2}}{\frac{2}{i} \frac{q^2}{q^2}} ; i = \pi, \rho, \omega, \rho' ; \quad (6)$$

where  $q$  and  $m_i$  are the four momentum and mass of the  $i$ th exchanged meson and  $\frac{2}{i}$  is the corresponding cut-off parameter. The latter governs the range of suppression of the contributions of high momenta which is done via the form factor. As before we take energy dependent meson-nucleon coupling constants of the following form

$$g(\frac{p}{s}) = g_0 \exp(-\frac{p}{s}) ; \quad (7)$$

This was found to be necessary to reproduce the NN scattering data in the entire range of beam energies [24]. The values of various parameters were the same as those used in the calculations reported in Refs. [24,27,29]. This ensures that the elastic NN elastic scattering channel remains the same in the description of various inelastic channels within this model, as it should be.

### B. Resonance-nucleon-meson vertex

In addition to nucleonic intermediate states (NN bremsstrahlung), we have considered in this work also the contributions from the (1232) isobar and N (1520) nucleon resonance intermediate states. The latter is a spin- $\frac{3}{2}$  negative parity resonance. While only and mesons couple to isobar, all of the four exchanged mesons, namely, , , !, and can couple to N (1520) resonance.

For spin- $\frac{3}{2}$  resonances, we use the following effective Lagrangians [35]

$$L_{RN} = \frac{g_{RN}}{m} \bar{R} \not{\partial}_N + H.c.: \quad (8)$$

$$L_{RN} = i \frac{g_{RN}}{m} \bar{R} (\not{\partial}_N \not{\partial}_N) + H.c.: \quad (9)$$

$$L_{RN!} = i \frac{g_{RN!}}{m!} \bar{R} (\not{\partial}_N \not{\partial}_N) + H.c.: \quad (10)$$

$$L_{RN} = \frac{g_{RN}}{m} \bar{R} (\not{\partial}_N) + H.c.: \quad (11)$$

Here,  $\bar{R}$  is the vector spinor for the spin- $\frac{3}{2}$  particle. In Eqs. [(8) – (11)], the operator is unity for even parity resonance and  $\gamma_5$  for the odd parity one, whereas  $\gamma_5$  for the even parity resonance and unity for the odd parity one. The meson fields in above equations need to be replaced by  $\not{\partial}_N$  (where corresponds to , , !, or meson fields) and  $T$  (where  $T$  and  $\not{\partial}_N$  are the isospin transition operator and Pauli isospin matrices, respectively) for isospin- $\frac{1}{2}$  and isospin- $\frac{3}{2}$  resonances, respectively.

The values of the coupling constants  $g_N$  and  $g_{N!}$  have been taken to be 2.13 and 7.14, respectively which are the same as those determined in Ref. [24] by fitting to experimental data on  $pp \rightarrow n \pi^{++}$  reaction at kinetic energies in the range of 1-2 GeV. We have assumed that the off-shell dependence of the resonance-nucleon vertex is determined solely by multiplying the vertex constant by a form factor. Similar to Ref. [24,27], we have used the following form factor for the vertices

$$F_i^N = \frac{(\not{q}_i)^2 - m_i^2 \not{\gamma}_2}{(\not{q}_i)^2 - \not{q}^2}; i = ; ; \quad (12)$$

with the values of the cut-off parameters as  $\not{q} = 1.421$  GeV, and  $\not{q} = 2.273$  GeV which are exactly the same as those used earlier [24,27,29].

For the  $N\bar{N}$  and  $N\bar{N}!$  vertices the coupling constants have been determined from the observed branching ratios for the decay of the resonance to  $N\bar{N}$  and  $N\bar{N}!$  channels, respectively. In the later case the finite lifetime for the decay  $N \rightarrow N!$  has been taken into account by introducing an integration over the corresponding phase space. The details of

this method are provided in Ref [29]. The values of the coupling constants so determined are  $g_{N\bar{N}} = 1.55$ , and  $g_{N\bar{N}^*} = 6.44$ . The coupling constants  $g_{N\bar{N}^*}$  and  $g_{N\bar{N}^*}$  are determined by vector meson dominance (VMD) hypothesis [36] and from the branching ratio of the decay of this resonance into the two pion channel [29], respectively. Their values are 3.42 and 1.24, respectively. It should be noted that there is considerable uncertainty in the latter two coupling constants. However, the contributions of these terms to the total dilepton production amplitude are almost negligible. As branching ratios determine only the square of the corresponding coupling constants, their signs remain uncertain in this method. Predictions from the independent calculations can, however, be used to constrain these signs [35,37,38]. Guided by the results of these studies, we have chosen the positive sign for the coupling constants for these vertices.

As in Refs. [35,36], we have used the following form factor for the  $N\bar{N}$  vertices

$$F_j^{N\bar{N}} = \frac{\left(\frac{N}{j}\right)^4}{\left(\frac{N}{j}\right)^4 + (q_j^2 - m_j^2)^2} ; j = 1, 2, 3 ; \quad (13)$$

with the value of the cut-off parameter being 0.8 GeV in all the cases. It may however be mentioned that identical results will be obtained if one uses the form factor as given by Eq. (12) with different cut-off parameters.

### C. Nucleon-nucleon-photon vertex

In the nucleonic bremsstrahlung process of dilepton production the intermediate nucleon is necessarily on-shell. The general form of the effective Lagrangian is given by

$$L_{N\bar{N}} = e A ; \quad (14)$$

where the half-on-shell nucleon-photon vertex function is [39{41]

$$= ie \sum_{s=1}^3 (F_1^s + F_2^s + F_3^s k) ; \quad (15)$$

In Eq. (15),  $k^2 = (p_f - p_i)^2$  with  $p_f$  and  $p_i$  being the initial and final nucleon four momenta.  $= (p + W) = W$  are the projection operators where  $W = (\not{p})^{1/2}$  and  $= i \not{k} = 2m_N$ . The form factors  $F_{1,2,3}$  are functions of  $k^2$ ,  $W$ , and  $m_N$ . The factor  $F_3$  is not independent but is constrained by the Ward-Takahashi identity [42] (i.e. by the requirement of gauge invariance)

$$F_1 = e_N + \frac{k^2}{W - m_N} F_3 ; \quad (16)$$

where  $e_N$  is the nucleon charge in units of  $e$ .

In this work, we have adopted the procedure followed in Refs. [24,43] where one uses the on-shell form of the vertex function also for the on-shell momenta. This means, one assumes  $F_1^+ = F_1^- = F_1$  and  $F_2^+ = F_2^- = F_2$  and  $F_3^+ = F_3^- = 0$ . This vertex does not in general satisfy gauge invariance. However, this can be achieved (see also [44]) by multiplying the external photon emission vertices by the same form factors that multiply

the hadronic vertices [Eq. (6)] and by multiplying the internal photon production diagram s by the following additional factor:

$$F_{\text{int}} = 1 + \frac{m_{\text{meson}}^2}{2} \frac{\vec{q}_1^2}{\vec{q}_1^2} + \frac{m_{\text{meson}}^2}{2} \frac{\vec{q}_2^2}{\vec{q}_2^2}; \quad (17)$$

where  $q_1$  and  $q_2$  are the four momentum transfers at the left and right vertices, respectively. In this way various electromagnetic form factors can be implemented for the hadrons without losing gauge invariance. Unfortunately, there are problems and ambiguities in the selection of form factors  $F_{1,2}$  (see e.g., [45] for a detailed discussion). It has been shown already in Ref. [24] that NN bremsstrahlung contributions depend sensitively on the choice of these form factors and that cross sections calculated with no form factors are closest to the data. In our calculations, we have used the prescription [35,45] of using no form factors at the electromagnetic vertices of the nucleon term and replacing  $F_1$  by the nucleon charge and  $F_2$  by nucleon anomalous magnetic moment.

#### D. Resonance-nucleon-photon vertex

For spin- $\frac{3}{2}$  resonance-nucleon- vertices, the form of the vertex functions is

$$V_{RN} = \frac{ie}{2m_N} g_1(k^2) + \frac{g_2(k^2)}{2m_N} p^i + \frac{g_3(k^2)}{2m_N} k^i (k^i g^j + k^j g^i) Z \quad (18)$$

where  $Z$  is 5 for the even parity resonance and unity for the odd parity one. Values of the coupling constants  $g_1$  and  $g_2$  are taken from table 4 of the first reference of [35]. The value of  $g_3$  was taken to be 7 for the isobar. For the case of N (1520), it was 1 and 3 for final nucleon being a proton or a neutron, respectively. The vertex function given by Eq. (18) fulfills gauge invariance [46] by the way of its construction.

It should be noted that the vector spinor vertices [Eqs. (8)–(11) and (18)] should in addition be contracted by an on-shell projector  $(z) = g - \frac{1}{2}(1 + 2z)$  where  $z$  is the on-shell parameter [35,47]. This operator describes the on-shell admixture of spin- $\frac{1}{2}$  fields [48]. The choice of the on-shell parameter  $z$  is arbitrary and it is treated as a free parameter to be determined by fitting the data. However, recently, the authors of Ref. [49] have proposed a different N interaction which leads to amplitudes where spin- $\frac{1}{2}$  components of the Rarita-Schwinger propagator (see in section E) drop out, thus making the on-shell parameters redundant (see, e.g., [45,49] for further details). The full implication of this prescription on observables calculated within the effective Lagrangian model will be investigated in future. In the present study we work with the couplings given by Eqs. (8)–(11) and (18).

#### E. Propagators

In the calculation of the amplitudes, the propagators for various mesons and nucleon resonances are required. For pion, meson and axial-vector mesons, they are given by

$$G(q) = \frac{i}{(q^2 - m^2)} \quad (19)$$

$$G(q) = i \frac{g}{q^2} \frac{q \cdot q = q^2}{m^2} \quad ! \quad (20)$$

$$G_A(q) = i \frac{g}{q^2 - m_A^2} \quad (21)$$

In Eq. (21), the mass of the axial meson is taken to be very large, as the corresponding amplitude is that of the contact term. The propagators for  $\pi$  and  $\rho$  mesons are similar to those given by Eqs. (20) and (19), respectively.

The propagator for the spin- $\frac{3}{2}$  resonance is

$$G_R(p) = \frac{i(p + m_R)}{p^2 - (m_R^2 - i(\Gamma_R/2))^2} \\ g \left[ \frac{1}{3} - \frac{2}{3m_R^2} p \cdot p + \frac{1}{3m_R^2} (p - p) \right]; \quad (22)$$

In Eqs. (22),  $\Gamma_R$  is the total width of the resonance which is introduced in the denominator term  $(p^2 - m_R^2)$  to account for the fact that the resonances are not the stable particles; they have a finite life time for the decay into various channels.  $\Gamma_R$  is a function of the center of mass momentum of the decay channel, and it is taken to be the sum of the widths for pion and rho decays (the other decay channels are considered only implicitly by adding their branching ratios to that of the pion channel)

$$\Gamma_R = \Gamma_{R\pi} + \Gamma_{R\rho} \quad (23)$$

The partial decay width  $\Gamma_{R\pi}$  is calculated in the same way as in Ref. [29]. This method is also identical to that used in Ref. [25]; the only difference is that while Ref. [29] uses a fully relativistic expression, that employed in [25] is its non-relativistic counterpart. For the partial width  $\Gamma_{R\rho}$ , we have used the same equations as given in Ref. [25] with identical values of all the parameters appearing therein.

#### F. Amplitudes and cross sections

After having established the effective Lagrangians, coupling constants and form of the propagators, we can now proceed to calculate the amplitudes for various diagrams associated with the  $N + N \rightarrow N + N + e^+ e^-$  reaction. These amplitudes can be written by following the well known Feynman rules [42] and calculated numerically. It should be stressed here that the signs of the various amplitudes are fixed, by those of the effective Lagrangians, coupling constants and the propagators as described above. These signs are not allowed to change anywhere in the calculations.

The general formula for the invariant cross section of the  $N + N \rightarrow N + N + e^+ e^-$  reaction is written as [50]

$$d = \frac{m_N^4 m_e^2}{2 \left[ (p_1^2 - p_2^2 - m_N^4) \right] (2\pi)^8} \frac{1}{4(p_f - p_i) \mathcal{A}_{fi} \int_{a=1}^{Y^4} \frac{d^3 p_a}{E_a}}; \quad (24)$$

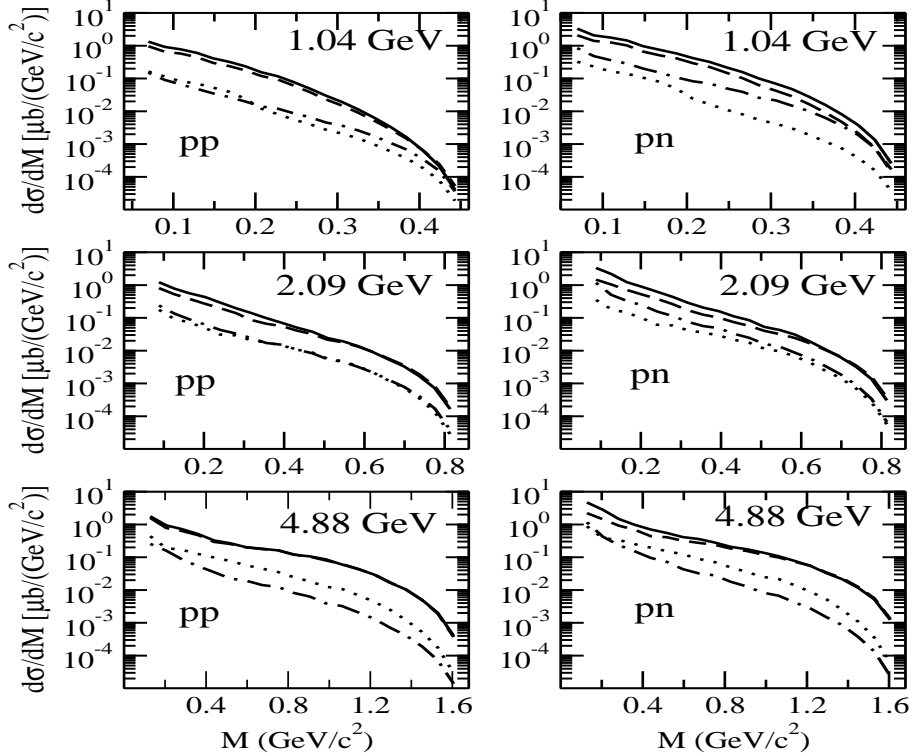


FIG. 2. Calculated invariant mass distributions for dileptons produced in proton-proton (left panel) and proton-neutron collisions (right panel) at the beam energies of 1.04 GeV, 2.09 GeV and 4.88 GeV. The contributions of the  $N\bar{N}$  bremsstrahlung (non-resonance), and the delta isobar and  $N$  (1520) resonance states are shown by dashed-dotted, dashed, and dotted lines, respectively. Their coherent sum is shown by solid lines.

where  $A_{fi}$  represents the total amplitude,  $P_i$  and  $P_f$  the sum of all the momenta in the initial and final states, respectively, and  $p_a$  the momenta of the particles in the final state. In Eq. (24)  $m_e$  represents the mass of the electron. The term  $jA_{fi}j$  already includes a sum over final spin and average over initial spin degrees of freedom of all particles.

### III. RESULTS AND DISCUSSIONS

In Fig. 2, we show the invariant mass spectra for dilepton production in both pp and pn collisions at bombarding energies of 1.04 GeV, 2.09 GeV and 4.88 GeV. It can be noted that in all the cases the dominant contribution arises from the intermediate states consisting of the isobar resonance. In fact the total yields are almost equal to the contributions of the amplitude alone. The pn cross sections are about a factor of 2-3 larger than those for the pp reactions even at the higher beam energy of 4.88 GeV. For beam energies of 1.04 GeV and 2.09 GeV, the contributions of the  $N$  (1520) terms are similar to those of the  $N\bar{N}$  bremsstrahlung processes for the pp collisions, while for the pn case the latter are larger than the former. However, at 4.88 GeV, the  $N$  channel prevails over the bremsstrahlung one in both cases. Any way, the isobar production terms are still dominant even at this high energy.

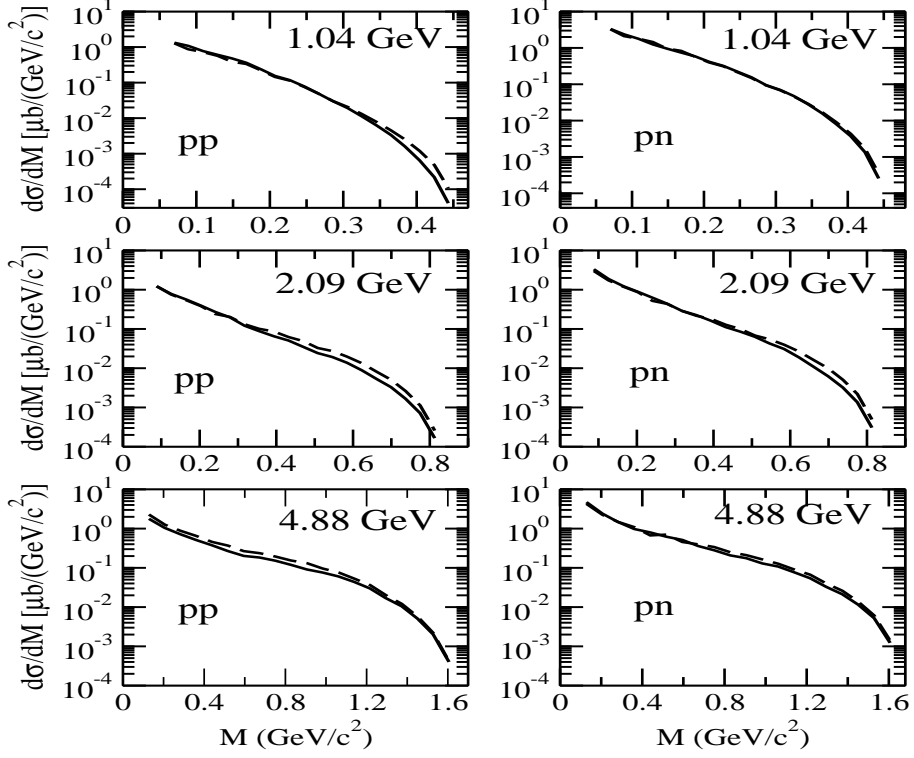


FIG. 3. Calculated invariant mass distributions for dileptons produced in proton-proton (left panel) and proton-neutron collisions (right panel) at the beam energies of 1.04 GeV, 2.09 GeV and 4.88 GeV. Solid and dashed lines show the cross sections obtained by coherent and incoherent sum mations of the amplitudes of various processes shown in Fig. 2, respectively.

The contributions of the nucleon bremsstrahlung process (graphs involving only intermediate nucleon lines) are considerably larger in case of pn reaction as compared to those for the pp case for all the beam energies. We do not observe the reversal of this trend at 4.88 GeV as seen in the soft-photon model calculations of Ref [23] (where NN bremsstrahlung is larger for pp reaction as compared to that for pn one). On the other hand, if the off-shell behavior of the effective NN interaction is described by using a T-matrix which includes the degrees of freedom, instead of the meson exchange mechanism as employed in our model, the pp bremsstrahlung contributions turn out to be larger than those of ours at the bombarding energy of 1 GeV. Yet due to lack of calculations for the pn case, it may not be possible to make comments about the relative pp and pn bremsstrahlung contributions within this approach. In any case, the coherent sum of the and bremsstrahlung terms as obtained within our model are similar to those calculated with the T-matrix method.

The role of the interference effects between various terms is investigated explicitly in Fig. 3 where we compare the cross sections obtained by coherent and incoherent sum mations of the amplitudes corresponding to various processes shown in Fig. 2. The former are the same as those shown by solid lines in Fig. 2. It is already noted in Fig. 2 that the delta contributions are slightly larger than the total ones at the larger mass end of the spectrum for all the beam energies in both the cases. In Fig. 3, one can further see that the interference effects are noticeable towards the larger mass ends of the spectra for beam energies below 4.88 GeV in case of pp collisions. For the 4.88 GeV case these effects show up also at lower

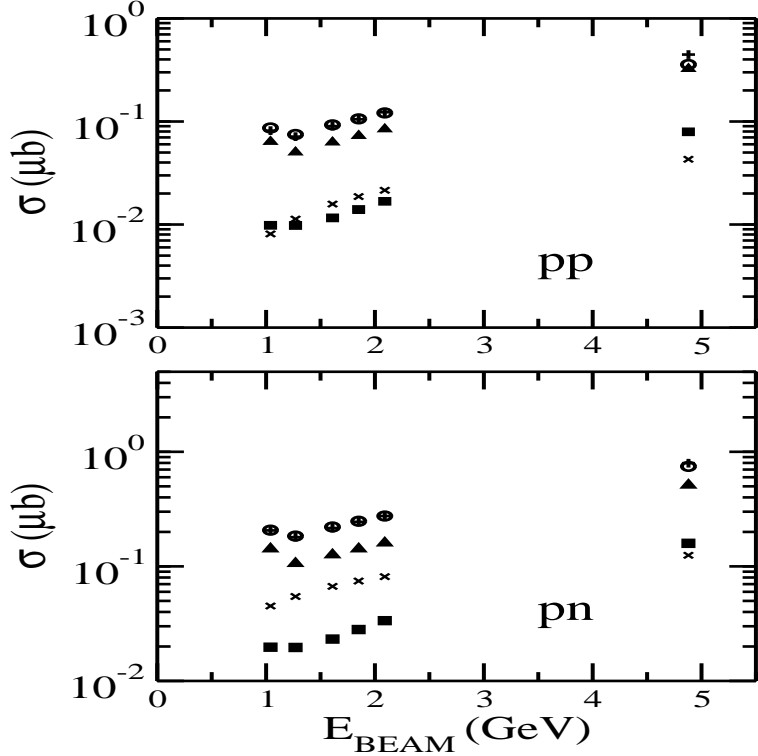


FIG. 4. Total dilepton production cross section in proton-proton (top) and proton-neutron (bottom) collisions as a function of beam energy. The nucleon, delta isobar and  $N$  (1520) contributions are shown by crosses, filled triangles and solid squares, respectively. The total cross sections obtained by coherent and incoherent summations of the corresponding amplitudes are shown by open circles and plus signs, respectively.

values of the invariant mass. On the other hand, they are relatively smaller for the pn case everywhere.

Contributions of various terms to the excitation function (integrated dilepton cross section) are shown in Fig. 4 for the pp (top) and pn (bottom) collisions. The total cross section at 1.04 GeV is slightly larger than that at 1.27 GeV in both the cases. However, after this it rises monotonously with the beam energy. The delta isobar terms dominate the total production yields for all the beam energies. For pp collisions,  $N N$  bremsstrahlung and  $N$  (1520) terms are of similar magnitude except at the beam energy of 4.88 GeV where the latter term is larger than the former. However, in the pn case, the  $N N$  bremsstrahlung contributions are larger than those of the  $N$  (1520) at lower beam energies while the two terms contribute similarly at 4.88 GeV. Furthermore, the difference in the interference effects of various terms in two cases, should also be noted. Cross sections obtained by coherent (shown by open circles) and incoherent (shown by plus signs) summations of the amplitudes differ very slightly for all the beam energies in case of the pn collisions and at energies smaller than 4.88 GeV for the pp case. This can be understood from the fact that the regions where the interference effects are visible in Fig. 3, contribute very little to the integrated cross sections for these cases. However, the interference effects do show up even in the total dilepton yields for pp collisions at 4.88 GeV beam energy.

The cross sections shown in Figs. 2 and 3 can not be compared straightforwardly with the

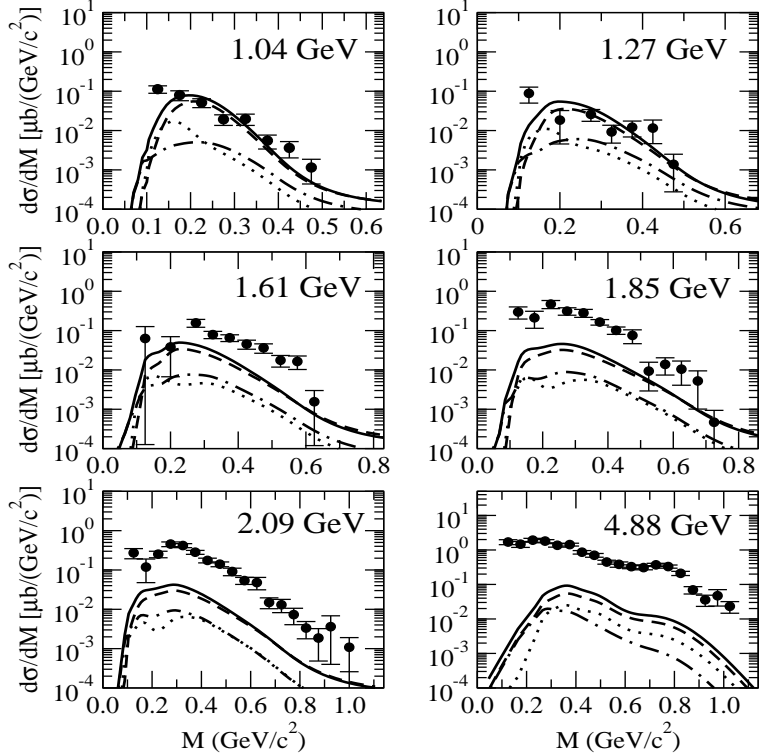


FIG. 5. Comparison of the effective Lagrangian model results for the invariant mass spectra of dileptons produced in proton-proton collisions, folded with the experimental filter, with the data of the DLS collaboration [33] at the beam energies of 1.04 GeV, 1.27 GeV, 1.61 GeV, 1.85 GeV, 2.09 GeV and 4.88 GeV. Various curves have the same meaning as in Fig. 2. The solid circles show the experimental data.

data of the DLS collaboration. They have to be folded with appropriate experimental filter, which is a function of the invariant mass ( $M$ ), transverse momentum ( $p_T$ ) and the rapidity in the laboratory frame ( $y_{lab}$ ) of the produced dileptons. We have used the DLS acceptance filter (version 4.1) in the folding procedure. In Fig. 5, we present a comparison of the folded invariant mass spectra (which also include the small mass resolution [25]) and the data from the DLS collaboration. We note that at the beam energies of 1.04 GeV and 1.27 GeV the effective Lagrangian model calculations are able to describe the data reasonably well in the region of  $M > 0.1$  GeV. However, at beam energies higher than 1.27 GeV, our calculations fail to reproduce the data, being lower than them by factors ranging from 2-20. Clearly, with increasing beam energy, other dilepton sources become important; these include Dalitz decays of hadrons ( $^0$ ,  $^+$  and  $^+$ ) [51,25,26], direct decay of  $^0$  and  $^+$  meson to dileptons, processes leading to multi-hadronic final states [23] and two pion annihilation [52]. Nevertheless, it is encouraging that the present effective Lagrangian model is able to account for the dilepton yields in pp collisions at beam energies around 1.0 GeV. Therefore, this theory could be useful in making predictions for the dilepton spectra to be measured by the HADES spectrometer at GSI, for beam energies in this region.

In order to study the role of other dilepton production processes not considered in the present effective Lagrangian model, we have included the contributions of the Dalitz decays:  $^0$   $^+$   $e^+ e^-$  and  $^+$   $e^+ e^-$ , and the direct decays  $^0$   $^+$   $e^+ e^-$  and  $^+ \bar{^+} e^+ e^-$ . The

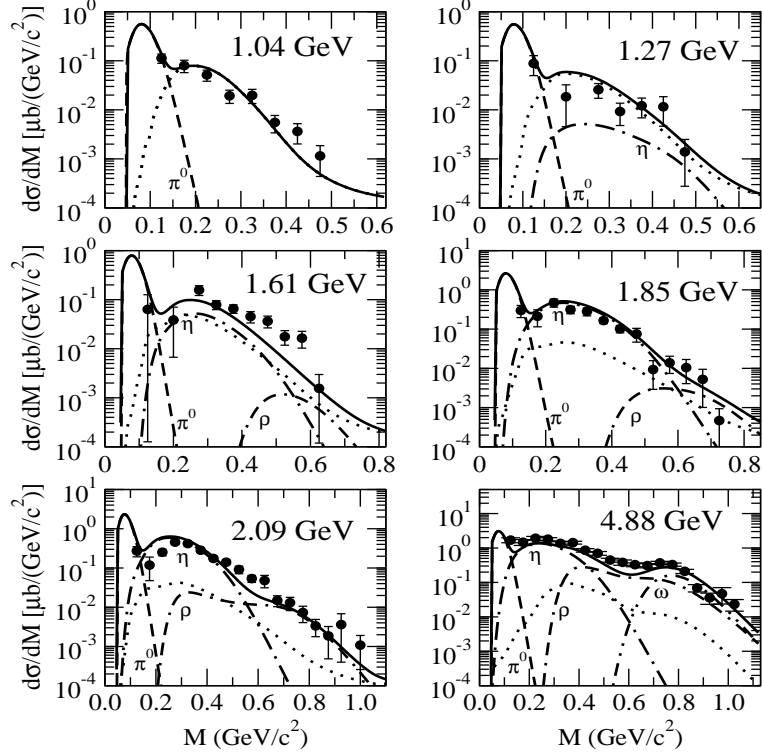


FIG. 6. The calculated dilepton invariant mass spectra for proton-proton collisions in the beam energy range of 1.04–4.88 GeV as comparison to the DLS data [33]. The effective Lagrangian model results are shown by the dotted lines (the same as those shown by full lines in Fig. 4. The contributions of  $\pi^0$ , Dalitz decay and  $\eta^0$  and  $\eta'$  direct decay processes are shown by dashed, dashed-dotted, dashed-dashed-dotted, and dot-dot-dashed lines, respectively. The incoherent sum of these cross sections with those of the effective Lagrangian model is shown by the solid line. Solid circles represent the experimental data.

details of these calculations are given in Ref. [25]. The cross sections of these processes were incoherently summed to those of the total mass differential cross sections (solid lines in Fig. 5) of the ELM. The results are shown in Fig. 6 together with the DLS data. It is clear that now the data can be described well for all the beam energies. This comparison suggests that the lowest points in the mass distributions of the dilepton stem from the  $\pi^0$  Dalitz decay. The Dalitz decay is important at the intermediate masses for beam energies between 1.61 GeV to 4.88 GeV, while  $\eta^0$  and  $\eta'$  direct decay processes are important at higher mass ends of the spectra for these beam energies. In addition to these processes, the multihadron final state bremsstrahlung mechanism could also contribute significantly in the low mass region at the beam energy of 4.88 GeV [23].

#### IV. SUMMARY AND CONCLUSIONS

We investigated the dilepton production in the nucleon-nucleon collisions at beam energies in the range of 1–5 GeV within an effective Lagrangian model, which is proven to describe well the pion and kaon production in  $N\bar{N}$  collisions. Most of the parameters of this

model are fixed by fitting to the elastic  $N\bar{N}$  T matrix; this restricts the freedom of varying the parameters of the model to provide a fit to the data. Along with the  $N\bar{N}$  bremsstrahlung process, the model also includes the excitation, propagation and radiative decay of  $(1232)$  and  $N(1520)$  intermediate nucleon resonant states. The coupling constants at vertices involving resonances have been determined from the experimental branching ratios of their decay into various relevant channels. The interference terms among various amplitudes are included in the total T matrix.

The reaction proceeds predominantly via excitation of the intermediate state in the entire beam energy range considered in this work. The contributions of  $N(1520)$  terms are relatively small. The  $N\bar{N}$  bremsstrahlung contributions are also weak in comparison to those of the delta isobar except for the higher mass region of the invariant mass spectra at the beam energy of  $1.04\text{ GeV}$ . In this region of these spectra considerable interference between various terms is also visible. For the case of pp collisions, the  $N\bar{N}$  bremsstrahlung and  $N(1520)$  contributions are similar in magnitude at lower beam energies. However, for the pn case, the former is larger than the latter at these energies. On the other hand, for the beam energies of  $4.88\text{ GeV}$ ,  $N(1520)$  terms are larger than those of the bremsstrahlung in both the cases. A key result of our study is that the pn bremsstrahlung is stronger than the pp one even at the beam energy of  $4.88\text{ GeV}$ .

At the lower beam energies ( $1.04\text{ GeV}$  and  $1.27\text{ GeV}$ ), the effective Lagrangian model calculations are able to explain the data of the DLS collaboration for the invariant mass distribution of dilepton emitted in pp collisions except for the lowest mass point. This is encouraging in the context of the analysis of the new experimental data on the dilepton production expected shortly from the HADES collaboration at GSI, Darmstadt.

However, at higher beam energies ( $1.61\text{ GeV}$ ,  $1.85\text{ GeV}$ ,  $2.09\text{ GeV}$  and  $4.88\text{ GeV}$ ), the effective Lagrangian model underpredicts the DLS data. This indicates that with increasing energy, other dilepton production sources become important. To stress this point further, we incoherently summed the  $^0$  and  $D$  Dalitz decay and  $^0$  and  $1$  direct decay contributions to the cross sections of the ELM. With this procedure, it is possible to provide a good description of the DLS data on the invariant mass distribution at all the beam energies. This also removes the discrepancy observed between the effective Lagrangian model calculations and the DLS invariant mass distribution data for the lowest mass point at the beam energies of  $1.04\text{ GeV}$  and  $1.27\text{ GeV}$ .

Our study has clarified the role of  $\Delta$  and  $N(1520)$  intermediate baryonic resonance states in the dilepton production in the  $N\bar{N}$  collisions. It also provides an indication of the direction in which the present effective Lagrangian approach should be improved. We require precise data where also the hadrons in the final channel are detected so that the role of various mechanisms in the dilepton production in nucleon-nucleon collisions can be investigated.

This work has been supported by the BMBF, Forschungszentrum Jülich, and GSI Darmstadt. One of the authors (RS) would like to thank Elena Bratkovskaya for several useful and clarifying discussions about the work presented in Refs. [25,26] and help in implementing the `lter` program of the DLS collaboration.

[1] C. Gale and J. Kapusta, *Phys. Rev. C* 35, 2107 (1987).

[2] L.H. Xia, C.M. Ko, L.X. Jiang and J.R. Wu, *Nucl. Phys. A* 485, 721 (1988).

[3] G.y. Wolf, G. Batko, W. Cassing, U. Mosel, K. Niita, and M. Schaefer, *Nucl. Phys. A* 517, 615 (1990).

[4] U. Mosel, *Annu. Rev. Nucl. Part. Sci.* 41, 29 (1991).

[5] G.E. Brown and M. Rho, *Phys. Rev. Lett.* 66, 2720 (1991).

[6] T. Hatsuda and S. Lee, *Phys. Rev. C* 46, R34 (1992).

[7] G. Chanfray and P. Schuck, *Nucl. Phys. A* 545, 271c (1992).

[8] M. Hermann, B. Friman, and W. Norenberg, *Nucl. Phys. A* 560, 411 (1993).

[9] M. Asakawa and C.M. Ko, *Phys. Rev. C* 48, R526 (1993).

[10] C.M. Shakin and W.D. Sun, *Phys. Rev. C* 49, 1185 (1994).

[11] F.K. Lingl and W. Weise, *Nucl. Phys. A* 606, 329 (1996); F.K. Lingl, N. Kaiser, and W. Weise, *ibid. A* 624, 527 (1997).

[12] R. Rapp, G. Chanfray, and J.W.ambach, *Nucl. Phys. A* 617, 496 (1997).

[13] S. Leupold, W. Peters, and U. Mosel, *Nucl. Phys. A* 628, 311 (1998).

[14] G.y. Wolf, W. Cassing, and U. Mosel, *Nucl. Phys. A* 552, 549 (1993).

[15] G. Akgichev et al., *Phys. Rev. Lett.* 75, 1272 (1995); Th. Ullrich et al., *Nucl. Phys. A* 610, 317c (1996).

[16] T. Akesson et al., *Z. Phys. C* 68, 47 (1995).

[17] G.Q. Li, C.M. Ko, and G.E. Brown, *Phys. Rev. Lett.* 75, 4007 (1995).

[18] C.M. Ko, G.Q. Li, and G.E. Brown, and H. Sorge, *Nucl. Phys. A* 610, 342c (1996).

[19] W. Cassing, W. Ehehalt, and C.M. Ko, *Phys. Lett. B* 363, 35 (1995); W. Cassing, W. Ehehalt, and I. Kralik, *ibid. B* 377, 5 (1996).

[20] E.L. Bratkovskaya and W. Cassing, *Nucl. Phys. A* 619, 413 (1997).

[21] W. Cassing, E.L. Bratkovskaya, R. Rapp, and J.W.ambach, *Phys. Rev. C* 57, 916 (1998).

[22] C. Gale and J. Kapusta, *Phys. Rev. C* 40, 2397 (1989).

[23] K. Haglin and C. Gale, *Phys. Rev. C* 49, 401 (1994).

[24] M. Schaefer, H.C. Donges, A. Engel, and U. Mosel, *Nucl. Phys. A* 575, 429 (1994).

[25] E.L. Bratkovskaya, W. Cassing, M. Ebenberger, and U. Mosel, *Nucl. Phys. A* 653, 301 (1999).

[26] E.L. Bratkovskaya, W. Cassing, and U. Mosel, *Nucl. Phys. A* 686, 568 (2001).

[27] A. Engel, R. Shyam, U. Mosel, and A.K. Dutt-Majumder, *Nucl. Phys. A* 603, 387 (1996).

[28] R. Shyam and U. Mosel, *Phys. Lett. B* 426, 1 (1998).

[29] R. Shyam, *Phys. Rev. C* 60, 055213 (1999); R. Shyam, G. Penner, and U. Mosel, *Phys. Rev. C* 63, 022202(R) (2001).

[30] F. de Jong and U. Mosel, *Phys. Lett. B* 379, 45 (1996);

[31] K.L. Haglin, *Annu. Phys.* 212, 84 (1991).

[32] A.I. Titov, B. Kamper, and E.L. Bratkovskaya, *Phys. Rev. C* 51, 227 (1995).

[33] W.K. Wilson et al., *Phys. Rev. C* 57, 1865 (1998).

[34] J.D. Bjorken and S.D. Drell, *Relativistic Quantum Mechanics* (McGraw-Hill, New York, 1964).

[35] T. Feuster and U. Mosel, *Nucl. Phys. A* 612, 375 (1997), *Phys. Rev. C* 58, 457 (1998), *Phys. Rev. C* 59, 460 (1999).

[36] M. Post and U. Mosel, *Nucl. Phys. A* 688, 808 (2001).

[37] D.M. Manley and E.M. Saleski, *Phys. Rev. D* 45, 4002 (1992).

[38] S. Capstick and W. Roberts, *Phys. Rev. D* 49, 4570 (1994).

[39] A.Yu. Korchin and O. Scholten, *Nucl. Phys. A* 581, 493 (1995).

[40] H.W. L.Naus and J.H. Koda, *Phys. Rev. C* 36, 2459 (1987).

[41] P.C. Tammiejer and J.A. Tjon, *Phys. Rev. C* 42, 599 (1990).

[42] C. Itzykson and J.B. Zuber, *Quantum Field Theory*, McGraw-Hill, New York, 1964).

[43] K. Haglin, J. Kapusta, and C. Gale, *Phys. Lett. B* 224, 433 (1989).

[44] I.S. Towner, *Phys. Rep.* 155, 263 (1987).

[45] G. Penner and U. Meißner, *Phys. Rev. C* 66, 055211 (2002); *Phys. Rev. C* 66, 055212 (2002).

[46] S. Nozawa, B. Blankleider, and T.-S.H. Lee, *Nucl. Phys. A* 513, 459 (1990); S. Nozawa and T.-S.H. Lee, *ibid A* 513, 511 (1990).

[47] M. Beznérrouche, N.C. Mukhopadhyay, and J.F. Zhang, *Phys. Rev. D* 51, 3237 (1995).

[48] M. Beznérrouche, R.M. Davidson, and N.C. Mukhopadhyay, *Phys. Rev. C* 39, 2339 (1989).

[49] V. Pascalutsa, *Phys. Rev. D* 58, 096992 (1998); V. Pascalutsa and

[50] M. Schäfer, T.S. Biro, W. Cassing, and U. Meißner, *Phys. Lett. B* 221, 1 (1989).

[51] C. Ernst, S.A. Bass, M. Belkadem, H. Stocker, and W. Greiner, *Phys. Rev. C* 58, 447 (1998).

[52] J. Kapusta and P. Lichard, *Phys. Rev. C* 40, R1574 (1989).